Motivations and Methods for Developing Nonlinear Near-field Acoustic Holography

Micah Shepherd, Kent L. Gee
Department of Physics and Astronomy
Brigham Young University

Abstract

Understanding the acoustic field radiated by finite-amplitude sources such as rockets and jets can be important for assessing the impact on involved structures and surrounding communities. Near-field acoustic holography techniques, based on linear equations, do not account for nonlinear behavior. A nonlinear study of the acoustic near-field is described using the general time domain algorithm. This algorithm accounts for all nonlinear phenomena involved. Nonlinear metrics, the bispectrum and Howell-Morfey nonlinearity indicator are being used to quantify the amount of nonlinear interactions occurring in the near-field. Analysis using these metrics is shown.

I. Introduction

Jets and rockets are an integral part of the advancing world of defense and aerospace technology. As they continue to become more powerful and valuable to our nation, noise problems could easily become worse than they currently are. Typical noise levels in areas of high jet and rocket activity are well above everyday OSHA work regulations. In fact, peak pressure levels from a rocket launch could easily be on the order of 10,000 Pa or one tenth of atmospheric pressure. Therefore, increased care must be taken to protect the surrounding community and environment from the harmful noise pollution.

Additionally, the high-amplitude pressure fields have an enormous impact on the structural integrity of the launch equipment and even on the aircraft itself. In order to determine the impact of the noise and structural vibrations, the characteristics of the sound source and general behavior of the acoustic radiation, including source location and strength, must be known.

Far-field measurements and other studies have shown some understanding of the complex behavior of the turbulence-induced acoustic fields. They have established that the sound source is directional and that the interactions creating the sound are located several meters downstream from the nozzle exhaust plume [1, 2]. However, for the most part these source mechanisms are not well understood and consequently are not able to be modeled accurately. For this reason, a method must be developed that can accurately characterize high-amplitude noise sources such as jets and rockets.

II. Theory

a) Near-field Acoustic Holography

Near-field acoustic holography (NAH) is a method similar to optical holography used to determine a 3-D

acoustic field quantity based on a 2-D pressure measurement [3]. Source characteristics can be determined using this method by measuring a planar array of pressure points (see Figure 1). NAH

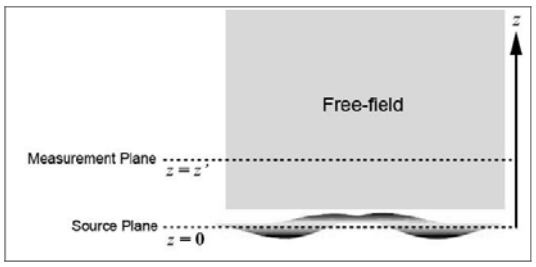

Figure 1) An array of pressure measurements can be used to determine radiating source characteristics

differs from other holographic techniques in that the holography plane must be in the acoustic near-field in order to have a good spatial resolution.

The NAH method is based on the linear Helmholtz equation,

$$\nabla^2 \hat{p} + k^2 \hat{p} = 0, \qquad (1.1)$$

where $\hat{p}$ is the acoustic pressure and k is the acoustic wave number, and uses Fourier techniques to propagate the measured pressure field back to the original source. The Helmholtz equation is a special time-harmonic case of the linear wave equation. This means that the acoustic waves propagate linearly with equal phase speed c, independent of amplitude. The linear assumption allows for superposition but is only valid for small-amplitude disturbances.

b) Nonlinear phenomenon

When sound fields have high amplitudes, higher-order terms that are negligible in small-amplitude acoustic disturbances are no longer negligible. The phase and wave speeds of the acoustic field are no longer equal and superposition does not apply. The amplitude-dependent phase speed causes the wave to travel faster at higher amplitudes. This causes an effective steepening of the waveform. Eventually this steepened waveform will become so

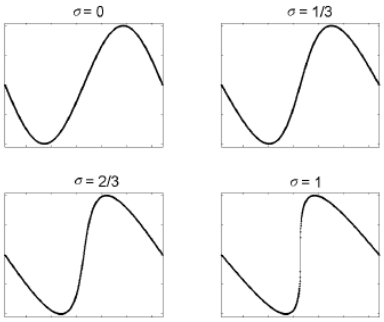

Figure 2) A nonlinear wave will become steepened as the high-amplitude sections of the wave travel faster than the low-amplitude sections. Eventually, a shock wave will form. σ represents the distance propagated normalized by the shock-formation distance.

steep that the waveform is no longer continuous and a shock wave is formed. The distance required for a lossless plane wave to form a shock wave is given as

$$\bar{x} = \frac{1}{\beta M k}, \qquad (1.2)$$

where β is the coefficient of nonlinearity, and M is the Mach number, defined as the peak particle velocity divided by the small signal sound speed [4]. Although this case is simple, it shows the general dependence of shock formation on frequency, Mach number and acoustic nonlinearity of the medium.

Physically, wave steepening can be interpreted as energy transfer from one frequency to another. Each energy transfer to a frequency would therefore appear to be radiated from a "virtual source" that is physically different in source strength as well as location than the original source. Also, a mean-flow

will be induced as the amplitude increases. This acoustic streaming effect has been shown to be present in the acoustic near-field of simple sources [5].

Additionally, losses become increasingly important as the acoustic wave steepens and forms shocks. Since the energy transfer is typically from lower frequencies to higher frequencies, the losses also must be accounted for correctly in order to attribute the right energy for the right frequency. These physical occurrences are not accounted for in the Helmholtz equation. Therefore, a nonlinear form of the lossy wave equation must be used.

III. Numerical Study of Nonlinearity

As previously described, a fully nonlinear wave equation must be solved in order to fully account for all physical phenomena that are occurring. Several nonlinear wave equations have analytical solutions. However, they all require assumptions that are not valid for this study. Therefore, numerical methods must be used to study nonlinear effects in the acoustic near-field of a source.

a) General Time Domain Algorithm

The General Time Domain Algorithm is an algorithm that accounts for these phenomena by solving the constitutive equations, a set of fully nonlinear equations governing fluid motion [6]. A form of this algorithm that can accurately account for wave steepening, shock formation and propagation, acoustic streaming and molecular and thermo-viscous losses has been used in this study.

The constitutive equations consist of the conservation of mass and momentum equations as well as the entropy-balance equation. They, in addition to the molecular relaxation equation are defined respectively as

$$\begin{aligned}
&\frac{D\rho}{Dt} + \rho\nabla\cdot\mathbf{v} = 0 \\
&\rho\frac{D\mathbf{v}}{Dt} = -\nabla\hat{p} + \nabla(\mu_B\nabla\cdot\mathbf{v}) + \mu\sum_{i,j} e_i \frac{\partial\phi_{i,j}}{\partial x_j} \\
&\rho\frac{Ds_{fr}}{Dt} + \sum_{\nu}\frac{\rho}{T_\nu}c_{\nu\nu}\frac{DT_\nu}{Dt} - \nabla\cdot\left(\frac{\kappa}{T}\nabla T\right) = \sigma_s \\
&\frac{DT_\nu}{Dt} = \frac{1}{\tau_\nu}(T - T_\nu)
\end{aligned} \qquad (2.1\text{-}4)$$

where, ρ is the fluid density, p is the acoustics pressure, **v** is the velocity vector, μ and μ_B are the shear and bulk viscosities, s_{fr} is the frozen entropy, T is the absolute temperature, κ is the coefficient of thermal conduction, $c_{\nu\nu}$ is the specific heat constant of the ν-type molecule, σ_s is the entropy source term, and T_ν and τ_ν are the apparent vibration temperature and relaxation time of the ν-type molecule. These equations can be solved in two-dimensional matrix form according to

$$\frac{\partial\mathbf{w}}{\partial t} + \frac{\partial\mathbf{F}}{\partial x} + \frac{\partial\mathbf{G}}{\partial y} = \mathbf{H} \qquad (2.5)$$

where **w** are the t-dependant terms, **F** are the x-dependant terms, **G** are the y-dependant terms, and **H** are the source terms defined as

$$\mathbf{w} = \begin{pmatrix} \rho \\ \rho u \\ \rho v \\ \rho s_{fr} \\ \rho T_{N_2} \\ \rho T_{O_2} \end{pmatrix} \quad \mathbf{F} = \begin{pmatrix} \rho u \\ \rho u^2 \\ \rho uv \\ \rho u s_{fr} \\ \rho u T_{N_2} \\ \rho u T_{O_2} \end{pmatrix} \quad \mathbf{G} = \begin{pmatrix} \rho v \\ \rho uv \\ \rho v^2 \\ \rho v s_{fr} \\ \rho v T_{N_2} \\ \rho v T_{O_2} \end{pmatrix} \qquad (2.5\text{-}7)$$

$$\mathbf{H} = \begin{pmatrix} 0 \\ -\frac{\partial \hat{p}}{\partial x} + \mu_B\left(\frac{\partial^2 u}{\partial x^2} + \frac{\partial^2 v}{\partial x \partial y}\right) + \mu\left(\frac{\partial \phi_{xx}}{\partial x} + \frac{\partial \phi_{xy}}{\partial y}\right) \\ -\frac{\partial \hat{p}}{\partial y} + \mu_B\left(\frac{\partial^2 v}{\partial y^2} + \frac{\partial^2 u}{\partial y \partial x}\right) + \mu\left(\frac{\partial \phi_{yx}}{\partial x} + \frac{\partial \phi_{yy}}{\partial y}\right) \\ \sigma_s - \sum_v \frac{\rho}{T_v} c_{vv} \frac{DT_v}{Dt} - \nabla \cdot \left(\frac{\kappa}{T} \nabla T\right) \\ \frac{\rho}{T_{N_2}}(T - T_{N_2}) \\ \frac{\rho}{T_{O_2}}(T - T_{O_2}) \end{pmatrix} \quad (2.8)$$

A third order Runge-Kutta technique is used in time and a Weighted-Essentially-Non-Oscillatory (WENO) method is used in space to solve equation 2.5. This method has been shown to accurately account for all phenomena that are important for this study (see [7] for details).

b) Nonlinearity Indicators

In order to assess the amount of nonlinear interactions in the field, two nonlinear indicators are being used as metrics, the bispectrum and the Howell-Morfey nonlinearity indicator, $Q_{p^2 p}$. Both show different information about the nonlinear interactions occurring in a time-waveform and therefore both are being used in this study.

The bispectrum, also called the bispectral density is defined as

$$S_{xxx}(f_1, f_2) = \lim_{T \to \infty} \frac{1}{T} E[X(f_1) X(f_2) X^*(f_1 + f_2)] \quad (3.1)$$

where $X(f_n)$ is the Fourier transform of the time signal $x(t_n)$ and E is the expected value operator. The bispectrum behaves similar to the power spectral density (PSD) but is dependent on two frequencies instead of just one.

The bispectrum for a statistically Gaussian signal is zero. Therefore a non-zero bispectrum can show non-Gaussian or nonlinear behavior. It can also show non-random phase relationships known as quadratic phase coupling. Quadratic phase coupling is an indication of second-order nonlinearity in a system that will shift energy to sum and difference frequencies. However, the bispectrum amplitude depends on several other complicated factors in the system. Therefore, a normalized version of the bispectrum called the bicoherence will be used. The bicoherence, $b(f_1, f_2)$, is defined as

$$b(f_1, f_2) = \frac{|S_{xxx}(f_1, f_2)|}{\sqrt{Z(f_1, f_2) S_{xx}(f_1 + f_2)}} \quad (3.2)$$

where Z(f) is the bifrequency spectral density defined as

$$Z(f_1, f_2) = E[|X(f_1) X(f_2)|^2] \quad (3.3)$$

and $S_{xx}(f_1 + f_2)$ is the power spectral density of $f_1 + f_2$. The numerator term will always be greater than the denominator term due to the Cauchy-Schwarz inequality, defined as

$$|E[\alpha\beta]|^2 \leq E[|\alpha|^2] E[|\beta|^2] \quad (3.4)$$

where $\alpha = X(f_1) X(f_2)$ and $\beta = X(f_1 + f_2)$. This forces the normalized bispectrum to a value between 0 and 1, where zero denotes no nonlinear interaction and one denotes high nonlinear interaction between those two frequencies [8].

The Howell-Morfey nonlinearity indicator, $Q_{p^2 p}$ is defined as the imaginary part of the cross spectral density between p and p^2. Its meaning comes from the Burgers equation, an approximation of the fully nonlinear

wave equation with an exact analytical solution, defined as

$$\frac{\partial \hat{p}}{\partial x} - \frac{\beta \hat{p}}{\rho c_0^{\,3}} \frac{\partial \hat{p}}{\partial t} = \frac{\delta}{2 c_0^{\,3}} \frac{\partial^2 \hat{p}}{\partial \tau^2} \quad (3.5)$$

Here, c_0 is the small signal sound speed, τ is the relaxation time and δ is the diffusivity of sound. After taking the Fourier transform and applying spherical spreading, equation 3.5 can be written as

$$(\frac{\partial}{\partial r} + \alpha')r\tilde{p} = j\omega \frac{\beta}{2\rho c_0^{\,3}} r\tilde{q} \quad (3.6)$$

where r is the radial distance, α' is the generalized absorption and dispersion coefficient, $\tilde{p}$ is the Fourier transform of the pressure and $\tilde{q}$ is the Fourier transform of the squared pressure. Multiplying r by the complex conjugate of the $\tilde{p}$ and taking the ensemble average of the real part yields

$$\frac{d}{dr}(e^{2\alpha x} S_p) = -\omega \frac{\beta}{2\rho c_0^{\,3}} e^{2\alpha x} Q_{p^2 p} \quad (3.7)$$

where S_p is the PSD and $Q_{p^2 p}$ is the imaginary part of the cross spectral density. For a linear system the spatial derivative of the PSD is zero. Therefore, $Q_{p^2 p}$ would account for any nonlinear effect causing the spatial derivative of the PSD to be non-zero. Thus, a positive value on the right-hand side of equation 3.7 would indicate energy gain at that frequency and distance, while a negative value would indicate energy loss or transfer [9].

IV. Model Jet Noise Analysis

The bispectrum and Howell-Morfey nonlinearity indicator were used in preliminary analysis of model jet noise measurements. These measurements give an indication of the behavior of a pressure field created by a small rocket launch. The metrics signify areas of high nonlinearity and low or negligible nonlinearity. This paper will only discuss how the previously mentioned metrics were used to assess nonlinearity and will not discuss the measurement set-up in detail or interpret other aspects of the data measurements. The measurements shown are at 140°, the angle of highest radiation, at a distance of 75 jet diameters from the source and at Mach numbers .85 and 2, representing low- and high-amplitude fields.

First, the normalized bispectrum is shown in figures 3 and 4. These graphs show nonlinear interactions between the frequencies on the x-axis with the frequencies on the y-axis. The lower values in the Mach .85 measurements show little nonlinear interactions while the higher values in the Mach 2 measurements indicate a lot of nonlinear interaction above 250 Hz.

The Howell-Morfey nonlinearity indicator is show in figures 5 and 6. The low Mach number measurements again show little nonlinear interactions while the higher Mach number shows more nonlinear energy transfer, with the highest amount of energy transfer being around 600 Hz. These two metrics therefore cam help quantify the amount of nonlinear interactions occurring in a waveform and contribute the overall understanding of the problem at hand.

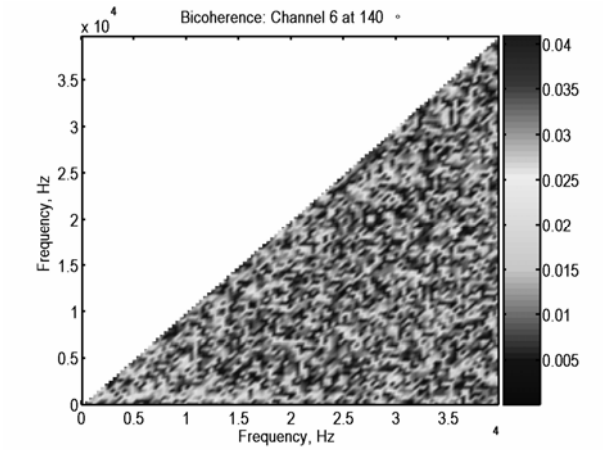

Figure 3) The bicoherence at 75 jet-diameters, 140°, and M=.85

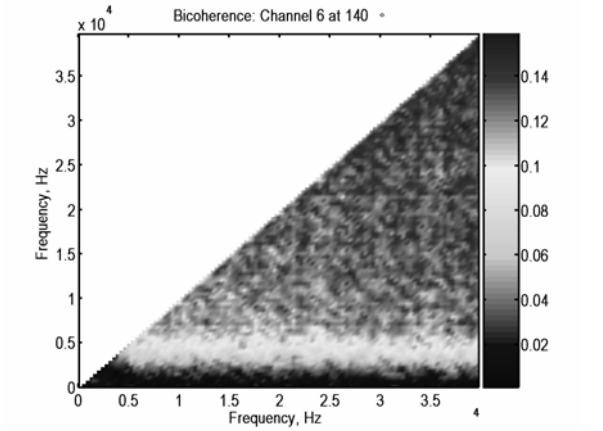

Figure 4) The bicoherence at 75 jet-diameters, 140°, and M=2

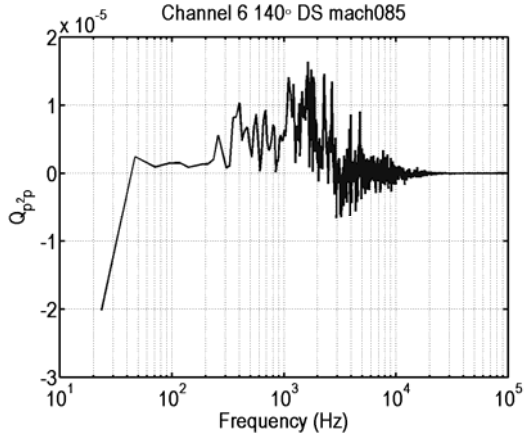

Figure 5) The Howell-Morfey indicator at 75 jet-diameters, 140°, and M=.85

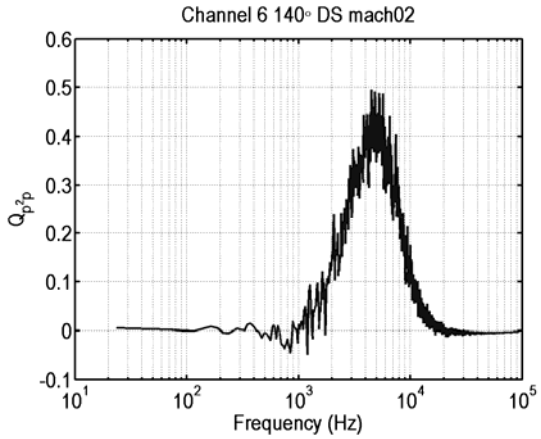

Figure 6) The Howell-Morfey indicator at 75 jet-diameters, 140°, and M=2.

V. Conclusions

The aeroacoustics industry would benefit greatly from being able to measure and know the radiation behavior of finite-amplitude sound sources. However, due to the complicated nature the nonlinear wave equation, numerical methods must be used to investigate this problem. A numerical method known as the general time domain algorithm is being used to study the nonlinearities present in the acoustic near-field of a source. The nonlinear interactions occurring are being studied using the bispectrum and the Howell-Morfey nonlinearity indicator. Using the information obtained from these studies and using linear NAH techniques, corrections factors will be determined for basic source configurations which will allow linear NAH techniques to be used to characterize finite-amplitude sound sources such as jets and rockets.

References

[1] MacInerny, S. (1990). Rocket Noise - A Review. *AIAA* 13th Aeroacoustics Conference

[2] Goldstein, M.E., (1976) *Aeroacoustics*. (McGraw-Hill International, New York).

[3] Maynard, J.D. Williams, E.G., and Lee, Y. (1985). Nearfield acoustic holography: I. Theory of generalized holography and the development of NAH. *J. Acoust. Soc. Am.* **78,** 1395-1413.

[4] Hamilton, M.F., and Blackstock, D.T., (1998). *Nonlinear Acoustics* (Academic Press, Chestnut Hill, MA)

[5] Yano, T., and Inoue, Y. (1996). Strongly nonlinear waves and streaming in the near field of a circular piston. *J. Acoust. Soc. Am.* **99,** 3353-3372. See also Yano, T., and Inoue, Y. (1994). Numerical study of strongly nonlinear acoustic waves, shock waves, and streaming caused by a harmonically pulsating sphere. *Phys. Fluids* **6,** 2831-2844.

[6] Sparrow, V.W., and Raspet, R. (1991). A numerical method for general finite amplitude wave propagation in tow dimensions and its application to spark pulses. *J. Acoust. Soc. Am.* **90,** 2683-2691.

[7] Wochner, M. (2006). Numerical Simulation of Multi-Dimensional Acousitc Propagation in Air Including the Effects of Molecular Relaxation. Ph.D. dissertation, The Pennsylvania State University.

[8] Gee, K.L., Atchley, A.A., Falco, L.E., Gabrielson, T.B., Sparrow, V.W. (2005). Bispectral Analysis of Jet Noise. *AIAA* 2937-2951.

[9] Falco, L., Gee, K.L., Atchley, A.A., Sparrow, V.W. (2005). Investigation of a Single-Point Nonlinearity Indicator in One-Dimensional Propagation. Proceedings of *ForumAcusticum 2005 Budapest*.